Title

Pittsburgh Compound-B (PiB) binds amyloid β-protein protofibrils

Permalink

https://escholarship.org/uc/item/70w4c2vn

Journal

Journal of Neurochemistry, 140(2)

ISSN

0022-3042

Authors

Yamin, Ghiam
Teplow, David B

Publication Date

2017

DOI

10.1111/jnc.13887

Peer reviewed

Pittsburgh Compound-B (PiB) binds amyloid β-protein protofibrils

Ghiam Yamin*,† and David B. Teplow†

*Department of Radiology, University of California San Diego School of Medicine, La Jolla, CA, USA

†Department of Neurology, David Geffen School of Medicine at UCLA, and Molecular Biology Institute (MBI) and Brain Research Institute (BRI), University of California, Los Angeles, CA, USA

Abstract

The neuropathology of Alzheimer's disease (AD) includes amyloid plaque formation by the amyloid β-protein (Aβ) and intracellular paired helical filament formation by tau protein. These neuropathogenetic features correlate with disease progression and have been revealed in brains of AD patients using positron emission tomography (PET). One of the most useful positron emission tomography imaging agents has been Pittsburgh Compound-B (PiB). However, since its introduction in 2002, substantial evidence has accumulated suggesting that Aβ oligomerization and protofibril formation, rather than fibril formation *per se*, may be the more important pathogenetic event in AD. Detecting protofibrils and oligomeric forms of Aβ thus may be of value. We report here the results of experiments to determine whether PiB binds to oligomers or protofibrils formed by Aβ40 and Aβ42. We observed strong binding to Aβ42 fibrils, significant binding to protofibrils, and weaker binding to Aβ42 oligomers. PiB also binds Aβ40 fibrils, but its binding to Aβ40 protofibrils and oligomers is substantially lower than for that observed for Aβ42.

Keywords: amyloid β-protein (Aβ), oligomers, Pittsburgh Compound-B (PiB), positron emission tomography (PET), protofibrils.

J. Neurochem. (2017) **140**, 210–215.

The most common late-life neurodegenerative disorder is Alzheimer's disease (AD). AD affects an estimated 5.3 million people in the US and 35 million people worldwide (Prince *et al.* 2013, Alzheimer's Association 2015). Unfortunately, no preventive, disease-modifying, or curative therapies currently exist (Cummings *et al.* 2014). AD is characterized histopathologically by the cerebral deposition of two hallmark proteinaceous aggregates: extracellular amyloid plaques formed by the amyloid β-protein (Aβ) and intracellular neurofibrillary tangles formed by tau protein (Goedert and Spillantini 2006). Aβ is produced through the endoproteolytic processing of the amyloid precursor protein by β-secretase and γ-secretase (O'Brien and Wong 2011), which leads to the formation of two predominant Aβ alloforms, Aβ40 (40 amino acids in length) and Aβ42 (42 amino acids in length). Aβ42 is more amyloidogenic than Aβ40 and is the predominant peptide found in neuritic plaques (Fukumoto *et al.* 1996), whereas Aβ40 is found in greater abundance in cerebrovascular amyloid (Smith and Greenberg 2009).

To date, no single test can identify a patient that has or will get AD. Instead, tests generally are used in combination to establish a diagnosis. These tests may include patient history and neuropsychological assessment (e.g., mini-mental status examination), CSF Aβ and tau concentrations, brain magnetic resonance imaging, and glucose positron emission tomography (PET) scans. However, even combinatorial testing does not provide a definitive diagnosis of AD (Khan and Alkon 2015). To improve diagnostic and prognostic capabilities, a number of PET imaging agents have been developed that bind to different amyloids (e.g., Aβ or tau) (Rowe and Villemagne 2011; Vlassenko *et al.* 2012; Mason *et al.* 2013). These include [18F]FDDNP, [11C]Pittsburgh Compound-B (PiB), [18F]Florbetapir (trade name: AMYViD), [18F]Florbetaben (trade name: Neuraceq), and [18F]

SHORT COMMUNICATION

Flutemetamol (trade name: Vizamyl) (Rowe and Villemagne 2011; Vallabhajosula 2011). These PET amyloid ligands provide semi-quantitative information about amyloid deposition in patients. Importantly, in some studies, evidence of amyloid deposition provided by these agents presaged the development of clinical symptoms of AD 7–15 years before their occurrence (Jack *et al.* 2013; Roe *et al.* 2013). This prognostic ability may provide a therapeutic window for secondary disease prevention not currently available.

PiB, a derivative of the fluorescent benzothiazole dye thioflavin T, binds to fibrillar Aβ, and thereby allows non-invasive visualization of amyloid deposits *in situ* (Klunk *et al.* 2004; Johnson *et al.* 2009). The Alzheimer's Disease Neuroimaging Initiative suggests that PiB is a useful predictor of cognitive decline and brain atrophy in patients with mild cognitive impairment (Weiner *et al.* 2010). However, working hypotheses about AD causation in which protofibrillar and oligomeric Aβ assemblies are the most important pathologic agents have supplanted those focusing solely on Aβ fibrils (Klein *et al.* 2004; Roychaudhuri *et al.* 2009; Kirkitadze *et al.* 2002; Haass and Selkoe 2007). PET imaging agents that bound these assemblies could have substantial clinical value. For these reasons, we evaluated the ability of PiB to bind Aβ protofibrils and oligomers.

Methods

Chemicals and reagents

[3]H-PiB, specific activity 72.44 Ci/mmol, and PiB were generously provided by Drs. Chet Mathis and William Klunk (University of Pittsburgh). Myoglobin (from horse skeletal muscle), albumin (chicken egg), insulin chain B (oxidized), and vitamin B12 were purchased from Sigma (Sigma-Aldrich, St. Louis, MO, USA). All solutions were prepared in double-distilled de-ionized (DDI) water produced using a Milli-Q system (Millipore Corp., Bedford, MA, USA).

Synthesis of Aβ

Aβ was synthesized, purified, and characterized essentially as described previously (Walsh *et al.* 1997). Briefly, peptide synthesis was performed on an automated peptide synthesizer (model 433A, Applied Biosystems, Foster City, CA, USA) using 9-fluorenyl-methoxycarbonyl-based methods on preloaded Wang resins. Aβ was purified to >97%, using reverse-phase high-performance liquid chromatography (HPLC). Quantitative amino acid analysis and mass spectrometry yielded the expected composition and molecular weight. Purified peptides were stored as lyophilizates at −20°C.

Preparation of Aβ for study

Aβ was prepared by dissolution in 10% (v/v) 60 mM NaOH, 45% (v/v) Milli-Q water, and 45% (v/v) 22.2 mM sodium phosphate, pH 7.5, to yield a nominal Aβ concentration of 1 mg/mL in 10 mM sodium phosphate, pH 7.5. The Aβ solution then was sonicated for 1 min in a bath sonicator (Branson Model 1510, Danbury, CT, USA) and filtered through a pre-washed 30 000 molecular weight cut-off Microcon centrifugal filter device (Millipore, Billerica, MA,

USA) for 15 min at 16 000 g. The eluate containing Aβ was quantified using UV absorbance ($\varepsilon_{280} = 1280$ cm^{-1} M^{-1}), using a 1 cm quartz cuvette (Hellma, Plainview, NY, USA) and a Beckman DU-640 spectrophotometer (Beckman Instruments, Fullerton, CA, USA), prepared with 10 mM sodium phosphate, pH 7.5. All measurements were performed at 22°C.

Preparation of Aβ oligomers, protofibrils, and fibrils

Oligomers and protofibrils were prepared according to Teplow *et al.* (Teplow 2006). Briefly, oligomers of Aβ40 and Aβ42 were prepared by dissolving 1 mg of Aβ peptide in 100 μL of 60 mM aqueous NaOH, 450 μL of water, and 450 μL of 22.2 mM sodium phosphate buffer, pH 7.5. The resulting solution, 10 mM sodium phosphate buffer, pH 7.5, was sonicated for 1 min in a bath sonicator (Branson Model 1510) and filtered through a pre-washed 30 000 molecular weight cut-off Microcon centrifugal filter device (Millipore) for 15 min at 16 000 g using a bench top centrifuge (model 5145C, Eppendorf, Hamburg, Germany) to remove insoluble material. Transmission electron microscopy (TEM) (Fig. 1) and size exclusion chromatography (SEC) confirmed the presence of oligomers. Oligomer size distributions and purities were also determined using photo-induced cross-linking of unmodified proteins, a zero-length chemical cross-linking method used to stabilize early Aβ assembly states, as previously published (Bitan *et al.* 2003).

Protofibrils were prepared following the procedure above, but after centrifugation, the supernates were transferred into fresh microcentrifuge tubes and incubated at 37°C for 48 h ([E22G] Aβ40) or 3 h ([E22G]Aβ42) without agitation. The respective [E22G]Aβ solutions then were centrifuged at 16 000 g for 10 min to pellet any fibrils present. The resulting supernates then were filtered through a Microcon centrifugal filter device (molecular mass cut-off of 30 kDa; Millipore, Billerica, MA, USA) to remove oligomers and monomers. The retentates were washed thrice with water and then resuspended in water at a concentration of 10 μM. EM confirmed the presence of protofibrils. The purities of the [E22G]Aβ40 and [E22G]Aβ42 protofibril preparations, determined using size exclusion chromatography (SEC), were 70% and 84%, respectively.

To prepare Aβ40 and Aβ42 fibrils, the procedure for preparing oligomers was followed, but after centrifugation, the resulting supernates were transferred into new microcentrifuge tubes and agitated with a mini rotator (Labnet International Inc., Edison, NJ, USA) using the rocking and tumbling function at 24 rpm at 37°C for 7 days. Thereafter, the resultant cloudy solution was centrifuged at 16 000 g for 10 min. The pelleted material was resuspended in 200 μL of 10 mM phosphate buffer, pH 7.5. EM confirmed the presence of fibrils.

Electron microscopy (EM)

Samples were prepared by spotting 5 μL of a 10 μM solution on to 300-mesh carbon-coated formvar copper grids (Ted Pella, Inc., Redding, CA, USA) for 20 min at 22°C, after which excess solution was wicked away with Whatman qualitative filter paper, grade 2 (Sigma-Aldrich). The grid then was incubated with 5 μL of 2.5% (v/v) glutaraldehyde in water for 5 min and the solution wicked away as previously described. Staining was done with 5 μL of 1% (w/v) uranyl acetate in water for 3 min. The stain was wicked off and the grid was air-dried. Images were obtained using
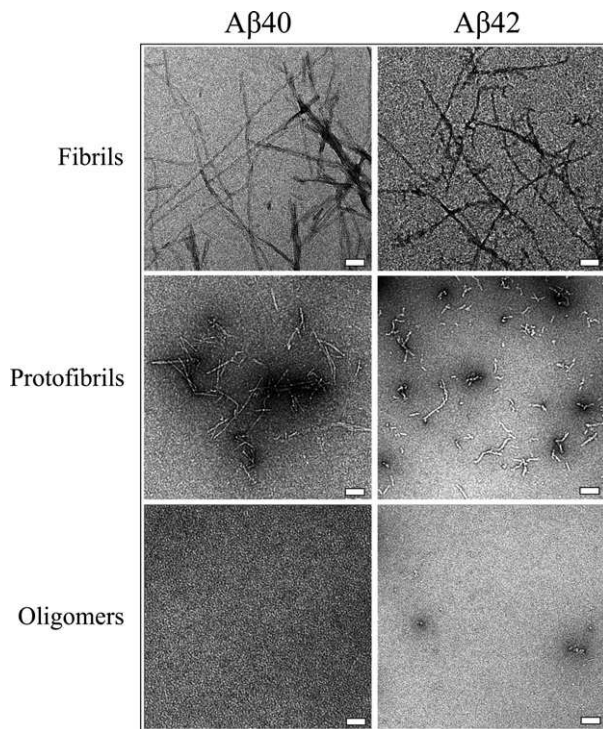
Fig. 1 Characterization of assembly morphology. Negative stain transmission electron microscopy (TEM) was performed on the following presumptive assemblies: Aβ40 fibrils; Aβ42 fibrils; [E22G] Aβ40 protofibrils; [E22G]Aβ42 protofibrils, Aβ40 oligomers, and Aβ42 oligomers. Blank grids display fine granular surfaces like those of the Aβ40 oligomer plate. White bar is 100 nm.

a Philips CM120 (FEI) transmission electron microscope equipped with a tungsten filament, operating at an accelerating voltage of 120 kV.

Size exclusion chromatography (SEC)

SEC, peak detection, and area calculations were performed on a Waters system (Waters Corp., Milford, MA, USA) comprising a 600S controller, 616 pump, 717plus autosampler, 486 Tunable Absorbance Detector, and PeakSimple Software (Waters Corp., Milford, MA, USA). Ten microliters of 4.26 mg/mL protein in 10 mM sodium phosphate, pH 7.4, was loaded onto a 7.8 × 300 mm SRT-SEC1000 column (5-μm particle size, 100 Å pore size; Sepax Technologies, Inc., Newark, DE, USA) fitted with a 7.8 × 50 mm SRT SEC-100 guard column (5-μm particle size, 100 Å pore size; Sepax Technologies, Inc.). The elution was carried out isocratically with 10 mM sodium phosphate buffer, pH 7.5, at 22.5°C at a flow rate of 0.5 mL/min and monitored by UV absorbance at 280 nm. Column standardization was done using a mixture of ovalbumin (65 kDa), myoglobin (17 kDa), oxidized insulin B-chain (3.5 kDa), and vitamin B12 (1.3 kDa).

Dot blotting and PiB binding

A range of concentrations of oligomeric, protofibrillar, and fibrillar Aβ, prepared in a fixed volume of 100 μL, were pipetted onto a polyvinylidene difluoride (PVDF) membrane (0.2-μm pore size) (Invitrogen, Carlsbad, CA, USA) and allowed to evaporate at 22.5°C

without suction (typically requiring < 30 min). Amino acid analysis of buffer washes/eluates of the protein-blotted PVDF membrane did not show presence of protein, suggesting that most, if not all, the material blotted onto membrane remained on the membrane.

The PVDF membrane then was placed in a BD Falcon Disposable Square Integrid Petri dish (BD Biosciences, Franklin Lakes, NJ, USA) and blocked with freshly prepared 5% (w/v) dry milk solution (2 mL) for 30 min. The membranes were then washed twice with 10 mM sodium phosphate, pH 7.4, for 30 min each time. Two milliliters of ^{3}H-PiB (3.4 nM) then was added and the blot was incubated at 37°C for 30 min, after which the blot was washed 4 × with 10 mM sodium phosphate buffer, pH 7.5, for 30 min each time. The membrane was air-dried overnight and then incubated in a Fujifilm BAS-TR 2025 Imaging Plate (FujiFilm, Tokyo, Japan) for 70 h along with two sets of tritium standards, 'low activity' standards with a specific activity range of 0.1-15.9 nCi/mg and 'high activity' standards with a range of 3.1-109 nCi/mg (American Radiolabeled Chemicals, Inc., St. Louis, MO, USA), and then analyzed with a Fujifilm BAS-5000 Imager (FujiFilm, Tokyo, Japan). These experiments were repeated three or more times using ^{3}H-PiB concentrations ranging from 0.1 to 7.5 nM (Fig. S1).

Results and discussion

Characterization of Aβ assembly structure by transmission electron microscopy (TEM)

The goal of our studies was to determine the binding specificity of PiB with respect to different biologically relevant Aβ assemblies. To do so, we first prepared and characterized the structures of oligomeric, protofibrillar, and fibrillar Aβ formed from Aβ40 and Aβ42. Protofibrillar Aβ assemblies were produced using Aβ40 and Aβ42 containing the 'Arctic' familial AD amino acid substitution E22→G (Nilsberth *et al.* 2001). This substitution produces Aβ peptides with high propensities for protofibril formation, but does not appear to significantly alter protofibril or fibril structure. TEM revealed that Aβ40 formed straight fibrils often comprising two twisted filaments with total width of 14.4 ± 1.6 nm and lengths greater than 1 μm (Fig. 1). Aβ42 fibrils had twisted morphologies, widths of 12.2 ± 0.8 nm, and lengths of 0.87 ± 0.43 μm. [E22G] Aβ40 samples comprised straight assemblies with widths of 10.9 ± 2.4 nm and lengths of 166.1 ± 66.9 nm. [E22G] Aβ42 samples showed straight and curved assemblies 7.4 ± 1.4 nm in width and 80.9 ± 36.1 nm in length. The morphological characteristics observed were consistent with those reported previously for Arctic protofibrils (Nilsberth *et al.* 2001). Low-molecular weight preparations of Aβ40 or Aβ42 contained no discernable assemblies.

Characterization of Aβ assembly structure by size exclusion chromatography (SEC)

We next used SEC to evaluate the size distributions of [E22G]Aβ40 and [E22G]Aβ42 assemblies separated and concentrated after incubation (see Methods). [E22G]Aβ40 produced three major peaks, at 13.3, 16.2, 17.2 min, and

minor peaks at 20.5, 23.4, and 25.5 min (Fig. 2, solid line). Assemblies completely excluded from the column matrix (void volume) elute at ≈12.5 min. The peak observed at 13.3 min, which constituted ≈70% of the total peak area in the chromatogram, is the protofibril peak (Walsh *et al.* 1999). Peaks at 16.2 and 17.2 min, corresponding to assemblies of 15.4 and 10.5 kDa molecular mass, accounted for ≈4% and ≈20% of the peak area, respectively. These peaks likely are low-order oligomers (dimers, trimers, tetramers) that form through dissociation of protofibrils during transit through the SEC column. This dissociation is expected, according to Le Châtelier's principle (Le Châtelier 1888), because protofibrils exist in equilibrium with oligomers and fibrils (Walsh *et al.* 1997). Peaks observed after 19 min correspond to UV-absorbing material too small to represent full-length Aβ monomers.

[E22G]Aβ42 produced a prominent peak at 13.4 min, which like the peak observed for [E22G]Aβ40 at 13.3 min, corresponds to the elution time for protofibrils (Fig. 2, dotted line). A smaller peak eluted at 12.5 min. These two peaks constituted ≈37% and ≈47% of the total peak area in the chromatogram, respectively. The elution time of the second peak suggests that this peak also contains protofibrils, but with conformations displaying somewhat higher Stokes radii. The EM data support this suggestion, as they showed that [E22G]Aβ42 produced two morphologically distinct populations of protofibrils, curved or straight. As with [E22G]Aβ40, species of substantially lower size also were observed, but in substantially lower amounts (peaks at 15.9 and

16.9 min). These peaks corresponded to analytes of molecular weight 17.3 and 11.7 kDa and accounted for ≈4% and ≈6% of the total peak area, respectively. The remainder of the total peak area after 19 min (≈6%) corresponds to UV-absorbing material of size too small to represent full-length Aβ monomers.

Analysis of PiB–binding specificity

To determine if PiB bound to oligomers or protofibrils, we dot blotted these assemblies, as well as fibrils, onto PVDF membranes. These membranes then were incubated with tritiated PiB (^{3}H-PiB), washed, and subjected to radiographic imaging (Fig. 3). Intense signals were recorded for all Aβ42 assemblies. Fibrillar Aβ42 displayed the highest ^{3}H-PiB binding, followed by Aβ42 protofibrils and then Aβ42 oligomers (Fig. 3, lanes 2, 4, and 6, respectively). Binding to Aβ40 assemblies also was observed, and with the same rank order of intensities relative to assembly state (Fig. 3, lanes 1, 3, and 5, respectively). However, for all these states, the absolute intensities were much lower than they were for Aβ42. For example, at 10 μg protein loading, the intensity of Aβ40 fibrils was ≈6-fold lower than that for Aβ42 fibrils (1114 vs. 6684 arbitrary units/mm^2) and the intensity of Aβ40 protofibrils was ≈13-fold lower than Aβ42 protofibrils (192 vs. 2439 arbitrary units/mm^2).

Signal intensity varied with sample loading. The data suggest that binding to fibrils saturates between 1 and 10 μg. The lowest signal intensities for both Aβ40 and Aβ42 fibrils were observed at 1 μg. However, we cannot determine

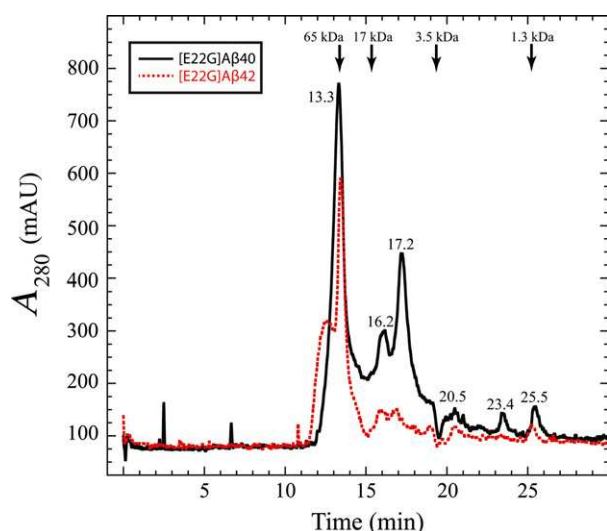**Fig. 2** Size exclusion chromatography (SEC). SEC was performed on 43 μg (10 μL of ≈4.3 mg/mL) of presumptive [E22G]Aβ40 (solid black line) and [E22G]Aβ42 (dotted red line) protofibrils (see Methods). Protein standards were albumin (65 kDa), myoglobin (17 kDa), insulin chain B (3.5 kDa), and vitamin B12 (1.3 kDa). The nominal separation range of the column is 100–100 000 Da. The void volume is ≈25 mL.
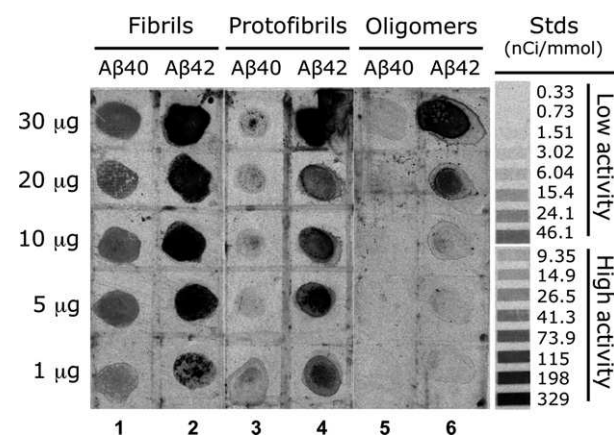

Fig. 3 ^{3}H-PiB binding to Aβ assemblies. Oligomeric, protofibrillar, and fibrillar Aβ assemblies were immobilized on polyvinylidene difluoride (PVDF) membranes, probed with ^{3}H-PiB, and then visualized by phosphorimaging. Lane 1, Aβ40 fibrils; lane 2, Aβ42 fibrils; lane 3, [E22G]Aβ40 protofibrils; lane 4, [E22G]Aβ42 protofibrils; lane 5, Aβ40 oligomers; lane 6, Aβ42 oligomers. Protein-only (no ^{3}H-PiB) and ^{3}H-PiB only (no protein) controls produced no signals (white background). Two specific activity (nCi/mmol) ranges of tritiated standards (Stds) are included at the right of the figure: 'low activity' (0.33–46) and 'high activity' (9.35–329).

whether the highest intensities occurred below or above 5 μg because signals at $\geq$ 5 μg were equal within experimental error. Binding of ^{3}H-PiB to Aβ40 protofibrils was maximal at 30 μg, a protein load at which signal saturation had not occurred. For Aβ42 protofibrils, signal intensity increased with amount of protein spotted and signal saturation occurred between 20 and 30 μg. These data show that the binding of ^{3}H-PiB to protofibrils, based on assembly weight, was lower than for fibrils. The lowest signal intensities were observed for stabilized Aβ oligomers. Weak binding was seen at 30 μg for Aβ40 oligomers. This intensity appears meaningful as no spots were observable at protein loads of 1–10 μg and a very faint spot was seen at 20 μg. A monotonic increase in signal intensity was seen for Aβ42 oligomers that had not saturated at 30 μg protein loading.

These findings are significant because they reveal that ^{3}H-PiB not only binds fibrils but also has the capacity to bind lower order assemblies, including Arctic Aβ42 protofibrils prepared *in vitro* and Aβ42 oligomers. Relative to fibrils, the binding of ^{3}H-PiB for Arctic protofibrils and oligomers is progressively lower. This may explain why ^{11}C-PiB binding was not observed in two patients with the Arctic form of early-onset AD (Schöll *et al.* 2012). The conformation of protofibrils in the Arctic patients also might be different from that of Arctic protofibrils produced *in vitro*. In this last respect, it is relevant that the terms 'protofibrils' and 'oligomers' are generic terms referring to two populations of assemblies that have been characterized primarily on the basis of their molecular weights and gross morphologies (Teplow 2013). Each population contains an indeterminate number of conformers, depending on the primary structure of the Aβ peptides from which the assemblies form and the conditions under which assembly occurs. An extensive determination of the binding affinities of PiB using a representative subset of each population would further our understanding of PiB-binding specificity.

Acknowledgments and conflict of interest disclosure

Supporting information

Additional Supporting Information may be found online in the supporting information tab for this article:

Figure S1. ^{3}H-PiB binding to Aβ protofibrils and fibrils.

References

Alzheimer's Association (2015) 2015 Alzheimer's disease facts and figures. *Alzheimers Dement.* **11**, 332–384.

Bitan G., Kirkitadze M. D., Lomakin A., Vollers S. S., Benedek G. B. and Teplow D. B. (2003) Amyloid β-protein (Aβ) assembly: Aβ40 and Aβ42 oligomerize through distinct pathways. *Proc. Natl Acad. Sci. USA* **100**, 330–335.

Cummings J. L., Morstorf T. and Zhong K. (2014) Alzheimer's disease drug-development pipeline: few candidates, frequent failures. *Alzheimers Res. Ther.* **6**, 37.

Fukumoto H., Asami-Odaka A., Suzuki N., Shimada H., Ihara Y. and Iwatsubo T. (1996) Amyloid β protein deposition in normal aging has the same characteristics as that in Alzheimer's disease. Predominance of Aβ42(43) and association of Aβ40 with cored plaques. *Am. J. Pathol.* **148**, 259–265.

Goedert M. and Spillantini M. G. (2006) A century of Alzheimer's disease. *Science* **314**, 777–781.

Haass C. and Selkoe D. J. (2007) Soluble protein oligomers in neurodegeneration: lessons from the Alzheimer's amyloid β-peptide. *Nat. Rev. Mol. Cell Biol.* **8**, 101–112.

Jack C. R. Jr, Wiste H. J., Lesnick T. G., *et al.* (2013) Brain β-amyloid load approaches a plateau. *Neurology* **80**, 890–896.

Johnson A. E., Jeppsson F., Sandell J., *et al.* (2009) AZD2184: a radioligand for sensitive detection of β-amyloid deposits. *J. Neurochem.* **108**, 1177–1186.

Khan T. K. and Alkon D. L. (2015) Alzheimer's disease cerebrospinal fluid and neuroimaging biomarkers: diagnostic accuracy and relationship to drug efficacy. *J. Alzheimers Dis.* **46**, 817–836.

Kirkitadze M. D., Bitan G. and Teplow D. B. (2002) Paradigm shifts in Alzheimer's disease and other neurodegenerative disorders: the emerging role of oligomeric assemblies. *J. Neurosci. Res.* **69**, 567–577.

Klein W. L., Stine W. B. Jr and Teplow D. B. (2004) Small assemblies of unmodified amyloid β-protein are the proximate neurotoxin in Alzheimer's disease. *Neurobiol. Aging* **25**, 569–580.

Klunk W. E., Engler H., Nordberg A., *et al.* (2004) Imaging brain amyloid in Alzheimer's disease with Pittsburgh Compound-B. *Ann. Neurol.* **55**, 306–319.

Le Châtelier H. L. (1888) Recherches expérimentales et théoriques sur les équilibres chimiques. *Ann. Min.* **13**, 157–380.

Mason N. S., Mathis C. A. and Klunk W. E. (2013) Positron emission tomography radioligands for in vivo imaging of Aβ plaques. *J. Labelled Comp. Radiopharm* **56**, 89–95.

Nilsberth C., Westlind-Danielsson A., Eckman C. B., *et al.* (2001) The 'Arctic' APP mutation (E693G) causes Alzheimer's disease by enhanced Aβ protofibril formation. *Nat. Neurosci.* **4**, 887–893.

O'Brien R. J. and Wong P. C. (2011) Amyloid precursor protein processing and Alzheimer's disease. *Annu. Rev. Neurosci.* **34**, 185–204.

Prince M., Bryce R., Albanese E., Wimo A., Ribeiro W. and Ferri C. P. (2013) The global prevalence of dementia: a systematic review and metaanalysis. *Alzheimers Dement.* **9**, 63–75, e62.

Roe C. M., Fagan A. M., Grant E. A., *et al.* (2013) Amyloid imaging and CSF biomarkers in predicting cognitive impairment up to 7.5 years later. *Neurology* **80**, 1784–1791.

Rowe C. C. and Villemagne V. L. (2011) Brain amyloid imaging. *J. Nucl. Med.* **52**, 1733–1740.

Roychaudhuri R., Yang M., Hoshi M. M. and Teplow D. B. (2009) Amyloid β-protein assembly and Alzheimer disease. *J. Biol. Chem.* **284**, 4749–4753.

Schöll M., Wall A., Thordardottir S., Ferreira D., Bogdanovic N., Langstrom B., Almkvist O., Graff C. and Nordberg A. (2012) Low PiB PET retention in presence of pathologic CSF biomarkers in Arctic APP mutation carriers. *Neurology* **79**, 229–236.

Smith E. E. and Greenberg S. M. (2009) β-Amyloid, blood vessels, and brain function. *Stroke* **40**, 2601–2606.

Teplow D. B. (2006) Preparation of amyloid β-protein for structural and functional studies. *Methods Enzymol.* **413**, 20–33.

Teplow D. B. (2013) On the subject of rigor in the study of amyloid β-protein assembly. *Alzheimers Res. Ther.* **5**, 39.

Vallabhajosula S. (2011) Positron emission tomography radiopharmaceuticals for imaging brain beta-amyloid. *Semin. Nucl. Med.* **41**, 283–299.

Vlassenko A. G., Benzinger T. L. and Morris J. C. (2012) PET amyloid-beta imaging in preclinical Alzheimer's disease. *Biochim. Biophys. Acta* **1822**, 370–379.

Walsh D. M., Lomakin A., Benedek G. B., Condron M. M. and Teplow D. B. (1997) Amyloid β-protein fibrillogenesis–Detection of a protofibrillar intermediate. *J. Biol. Chem.* **272**, 22364–22372.

Walsh D. M., Hartley D. M., Kusumoto Y., Fezoui Y., Condron M. M., Lomakin A., Benedek G. B., Selkoe D. J. and Teplow D. B. (1999) Amyloid β-protein fibrillogenesis–Structure and biological activity of protofibrillar intermediates. *J. Biol. Chem.* **274**, 25945–25952.

Weiner M. W., Aisen P. S., Jack C. R., *et al.* (2010) The Alzheimer's disease neuroimaging initiative: progress report and future plans. *Alzheimers Dement.* **6**, 202–211, e207.

SUPPORTING INFORMATION

Pittsburgh Compound-B (PiB) binds amyloid β-protein protofibrils

Ghiam Yamin[1, 2] and David B. Teplow[2]*

[1]Department of Radiology, University of California San Diego School of Medicine, La Jolla, CA; [2]Department of Neurology, David Geffen School of Medicine, and Molecular Biology Institute (MBI) and Brain Research Institute (BRI), University of California, Los Angeles, Los Angeles, CA

Fig. S1. ^{3}H-PiB binding to Aβ protofibrils and fibrils. A PVDF membrane was fixed in a Bio-Dot apparatus containing a 96-well sample template, vacuum manifold base, gasket support plate, and gasket (Bio-Rad Laboratories, Life Science Research, Hercules, CA). The membrane then was washed with 100% methanol and dried. Twenty μL of protofibrillar or fibrillar Aβ (0.91 μg of Aβ40 and 0.95 μg of [E22G]Aβ42) were introduced into wells in the apparatus and then dried under vacuum at 22.5°C (typically requiring <30 min), probed with 200 μL of ^{3}H-PiB ranging in concentration from 0.1 to 7.5 nM, and then visualized by phosphorimaging. Lane 1, [E22G]Aβ40 protofibrils; lane 2, [E22G]Aβ42 protofibrils; lane 3, Aβ40 fibrils; lane 4, Aβ42 fibrils. Protein-only (no ^{3}H-PiB) and ^{3}H-PiB only (no protein) controls produced no signals (white background). Two specific activity (nCi/mmol) ranges of tritiated standards (Stds) are included at the right of the figure: "low activity" (0.33-46) and "high activity" (9.35-329).

Protofibrils Fibrils Stds
(nCi/mmol)

Aβ40 Aβ42 Aβ40 Aβ42

[³H-PiB]

7.5 nM

3.0 nM

1.0 nM

0.5 nM

0.2 nM

0.1 nM

0.33
0.73
1.51
3.02
6.04
15.4
24.1
46.1

Low Activity

329
198
115
73.9
41.3
26.5
14.9
9.35

High Activity